Supporting Information

Rationally Tailored Redox Property of a Mesoporous Mn-Fe Spinel Nanostructure for Boosting Low-Temperature Selective Catalytic Reduction of NO_x with NH_3

Liehao Wei[a], Xinyong Li[*a,b], Jincheng Mu[a], Xinyang Wang[a], Shiying Fan[a], Zhifan Yin[a], Moses O. Tadé[b] and Shaomin Liu[b,c]

[a] *State Key Laboratory of Fine Chemicals, Key Laboratory of Industrial Ecology and Environmental Engineering (MOE), School of Environmental Science and Technology, Dalian University of Technology, Dalian 116024, China*

[b] *Department of Chemical Engineering, Curtin University, GPO Box U1987, Perth, WA 6845, Australia*

[c] *College of Chemical Engineering, Beijing University of Chemical Technology, Beijing 100029, PR China*

*Corresponding author

Tel: +86-411-8470-6658;

E-mail: xyli@dlut.edu.cn

Number of pages: 20

Number of figures: 16

Number of tables: 2

1. EXPERIMENTAL SECTION

1.1. Catalyst Preparation.

The $Mn_{0.5}Fe_{2.5}O_4$-S sample with a mesoporous nanosphere was synthesized by a solvothermal method.[1] In a typical process, 16 mL of glycerol and 80 mL of isopropanol were thoroughly mixed, to form a homogeneous transparent liquid. Then 0.125 mmol of $Mn(NO_3)_2{\cdot}6H_2O$ and 0.625 mmol of $Fe(NO_3)_3{\cdot}9H_2O$ were added into the above solution along with intensely stirring. After stirring for 15 minutes, the mixed solution was transfer into Teflon-lined stainless steel autoclave (100 mL) and kept at 180 ℃ in oven for 6 h. The claybank precipitate was washed with ethanol for several times by centrifugation and dried at 60 ℃ in a vacuum oven overnight. Finally, the precursor was annealed at 400 ℃ for 2 h with a heating rate of 20 ℃·min^{-1} in air. γ-Fe_2O_3 (denoted as Fe_2O_3-S) was obtain by the similar procedure without the presence of $Mn(NO_3)_2{\cdot}6H_2O$. Besides, the $Mn_{0.5}Fe_{2.5}O_4$-S catalysts powders and pseudo-boehmite (the mass ratio is 3:1) as the raw materials, and 6.8vol% nitric acid as the adhesive solvent, to synthesize the tube-like monolithic catalysts precursor. Then, the precursor was dried and annealed with the same condition, to synthesize the tube-like monolithic $Mn_{0.5}Fe_{2.5}O_4$-S (denoted as $Mn_{0.5}Fe_{2.5}O_4$-S_M).

For comparison, the $Mn_{0.5}Fe_{2.5}O_4$ nanoparticle catalyst (denoted as $Mn_{0.5}Fe_{2.5}O_4$-P) was prepared by a conventional co-precipitation method.[2] Appropriate amounts of $Fe(NO_3)_3{\cdot}9H_2O$, $FeSO_4$, and $Mn(NO_3)_2{\cdot}6H_2O$ were dissolved in deionized water (total cation concentration = 0.30 mol·L^{-1}). Then, sodium hydroxide solution with the concentration of 1.2 mol·L^{-1} was prepared. The above two solutions are thoroughly mixed, resulting in a transient precipitation of manganese ferrite in 15 minutes. The black precipitate was collected by centrifugation, and

washed with deionized water for several times until the water is neutral. Finally, the particles were dried at 105 ℃ in a vacuum and annealed in the same conditions.

1.2. Catalyst Characterization.

Thermogravimetry (TG) analysis was procured from the instrument (EXSTAR 6300) producted by Lenovo (Beijing) Limited co., Itd. In the air, the sample went through heat treatment from room temperature to 500 ^{o}C with a heating rate of 20 ^{o}C·min^{-1}. Scanning electron microscopy (SEM) images were obtained from a Hitachi SU8010 apparatus. The structure of materials and distribution of elements were captured by transmission electron microscopy (TEM) and the energy dispersive X-ray spectrometer (EDS) respectively by using a FEI Tecnai G20 with 200 kV voltages. X-ray diffraction (XRD) patterns were performed by a D/Max 2400 X-ray power diffractometer with Cu K_{α} radiation in the range from 10 ° to 80 °. The NOVA 4200e automated surface area and pore size analyzer was utilized to obtain the N_2 adsorption-desorption isotherms of materials at 77 K. The specific surface were calculated by Brunauer-Emmett-Teller (BET) method and the average pore diameters and pore volumes were calculated by using the Barrett-Joyner-Halenda (BJH) method from the desorption branch of the isotherms. X-ray photoelectron spectroscopy (XPS) was recorded on a Thermo ESCALAB 250Xi multifunctional imaging electron spectrometer using a monochromatic Al Ka radiation. The binding energy of Fe 2p, Mn 2p and O 1s were calibrated using C 1s (BE = 284.6 eV) as standard. The temperature-programmed reduction of H_2 (H_2-TPR) was performed on a Chembet PULSAR TPR/TPD analyzer. Before experiment, 30 mg of catalyst was pretreated at 200 ℃ for 30 min in a He flow. After cooling to room temperature, the TPR measurement was implemented from room temperature to 900 ℃ with a ramping rate of 10 ℃·min^{-1} and the consumption of H_2 was detected by a thermal conductivity detector.

1.3. Catalytic Activity Experiments.

Activity measurements *X* were implemented in a fixed-bed reactor with U-tube quartz (4mm i.d.). The reaction gas includes 500 ppm NO_x, 500 ppm NH_3, 5% O_2, 50 ppm SO_2 (when used), 5vol% H_2O (when used), and Ar balance with a total flow rate of 200 $mL \cdot min^{-1}$. 260 mg of each catalyst (20-40 mesh) was used for activity measurements with a gas hourly space velocity (GHSV) of 50000 h^{-1}. The concentration of the NO and NO_2 in both feed gas and the effluent streams were analyzed by an online gas analyzer (Testo 350). The concentration of N_2 in the outlet gas were scaled by a gas chromatography (Techcomp 7890II). The NO_x conversion and N_2 selectivity were calculated according to the following equations, respectively.

$$NO_x \text{ conversion } (\%) = \frac{[NO_x]_{in} - [NO_x]_{out}}{[NO_x]_{in}} \times 100\% \quad \text{(S1)}$$

$$N_2 \text{ selectivity } (\%) = \frac{2[N_2]_{out}}{[NO_x]_{in} - [NO_x]_{out} + [NH_3]_{in} - [NH_3]_{out}} \times 100\% \quad \text{(S2)}$$

$$NO \text{ conversion } (\%) = \frac{[NO]_{in} - [NO]_{out}}{[NO]_{in}} \times 100\% \quad \text{(S3)}$$

Where $[NO_x] = [NO] + [NO_2]$, and the $[NO]_{in}$ and $[NO]_{out}$ indicated the inlet and outlet concentration at steady state, respectively.

The normalized reaction rate (*k*, $cm^3 \cdot m^{-2} \cdot s^{-1}$) was figured through the eq 4 by using NO_x conversion below 15% to exclude the effect of both thermal and diffusion. The apparent activation energies (E_a) were obtained from the slop of linear plot of ln(R) versus 1000/T according to Arrhenius law (eq 5).[3]

$$k = -\frac{VC}{MS}\ln(1 - X) \quad \text{(S4)}$$

$$k = A \exp\left(\frac{-E_a}{RT}\right) \quad \text{(S5)}$$

Where M is the mass of each catalyst (g), S is BET surface area ($m^2 \cdot g^{-1}$), V is total flow rate ($cm^3 \cdot s^{-1}$), C is the concentration of NO_x, X is the conversion of inlet NO_x, and R is ideal gas constant (R = 8.314).

1.4. In Situ DRIFTS Studies.

The NH_3/NO+O_2 adsorption and SCR reaction process on the catalysts were investigated through in situ DRIFTS analysis undertaken with a VERTEX 70-DRIFTS (Bruker). Before each experiment, the catalyst was pretreated in a flow of Ar at 300 ℃ for 60 min, and cooled to the desired temperature to obtain the corresponding background spectra, which was automatically subtracted from the sample spectra in the following testing process. For each experiment, the reaction condition were 500 ppm of NH_3, 500 ppm of NO, 5 vol % O_2, and Ar balance and the total flow rate was kept at 100ml·min^{-1}.

1.5. DFT Calculations.

The dehydrogenation of NH_3 and oxidation of NO on $Mn_{0.5}Fe_{2.5}O_4$ surface were investigated by the Vienna Ab-initio Simulation Package (VASP) using the revised Perdew-Burke-Ernzerhof (RPBE) of the generalized gradient approximation (GGA). The PAW pseudo-potential was used to describe the interaction between valence electrons and ionic. The $Mn_{0.5}Fe_{2.5}O_4$ surface was simulated by the typical 2 × 2 (110) and (311) supercells with the approximate atomic thickness of 10 Å. The energy convergence of 1.0×10^{-4}eV and the cutoff energy of 400 eV were used to perform all geometry at gamma point, which obtained the initial state and final state of following transition state. The transition state calculation was conducted by the climbing nudged elastic band (Cl-NEB). The convergence threshold of force was set to 0.05 eV/Å, respectively. The adsorption energy (E_{ads}) denoted the interaction between the surface and the adsorbate, which is defined as: $E_{ads} = E_{total} — E_{sub} — E_c$. Where E_{total} is the total energy of the system; E_c and E_{sub} are the energy of the catalyst model and gas molecule, respectively. The NEB path was described by four elementary steps in the all searches of transition state.

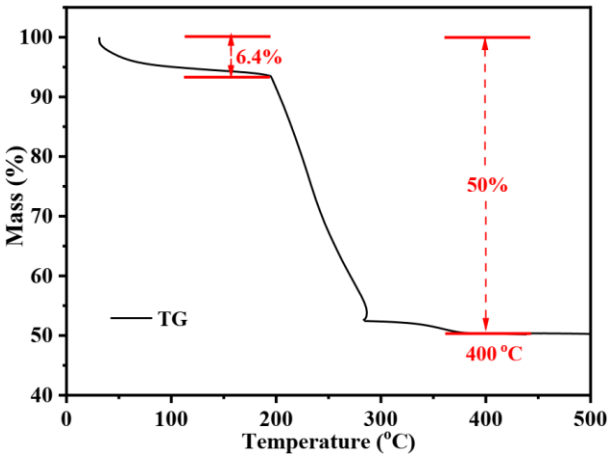

Figure S1. TG analysis curve of the precursor manganese-iron glycerate (MnFe-glycerate).

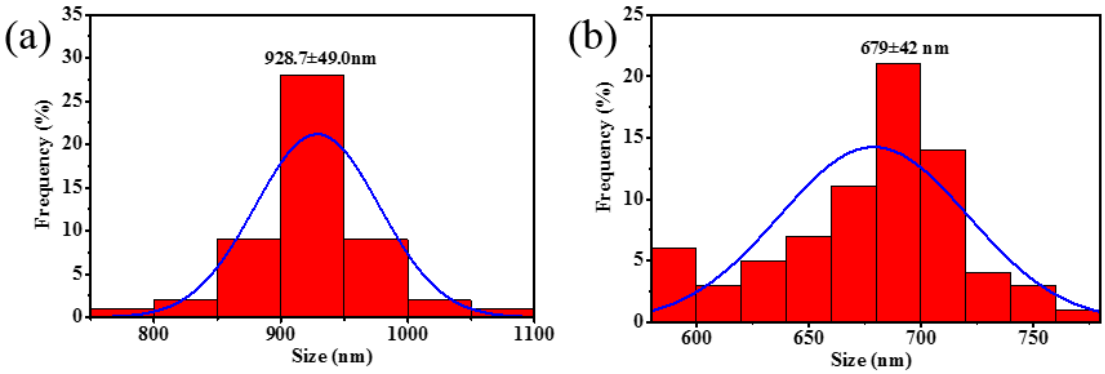

Figure S2. The particle size analysis chart of (a) precursor and (b) $Mn_{0.5}Fe_{2.5}O_4$-S.

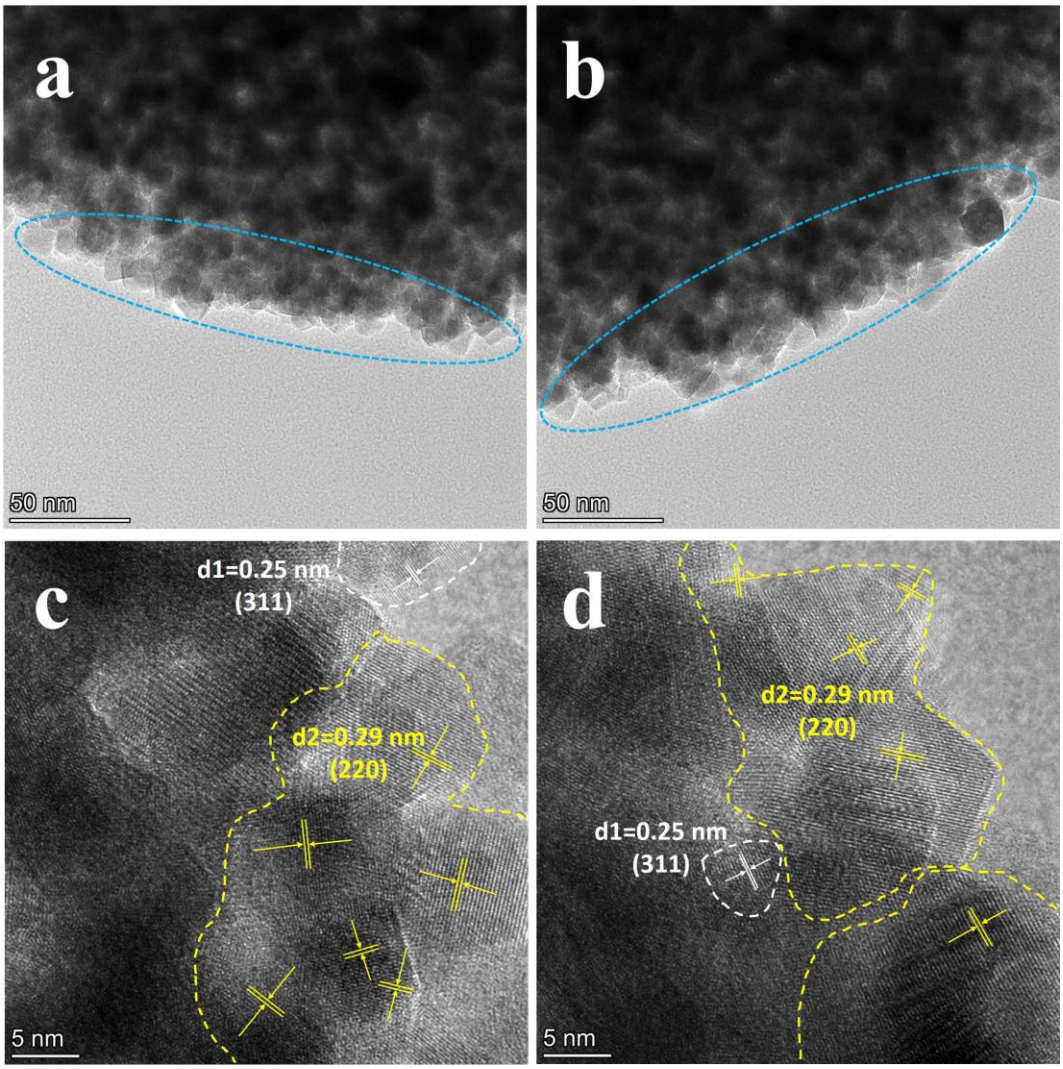

Figure S3. (a-b) TEM images, (c-d) HRTEM images of $Mn_{0.5}Fe_{2.5}O4$-S.

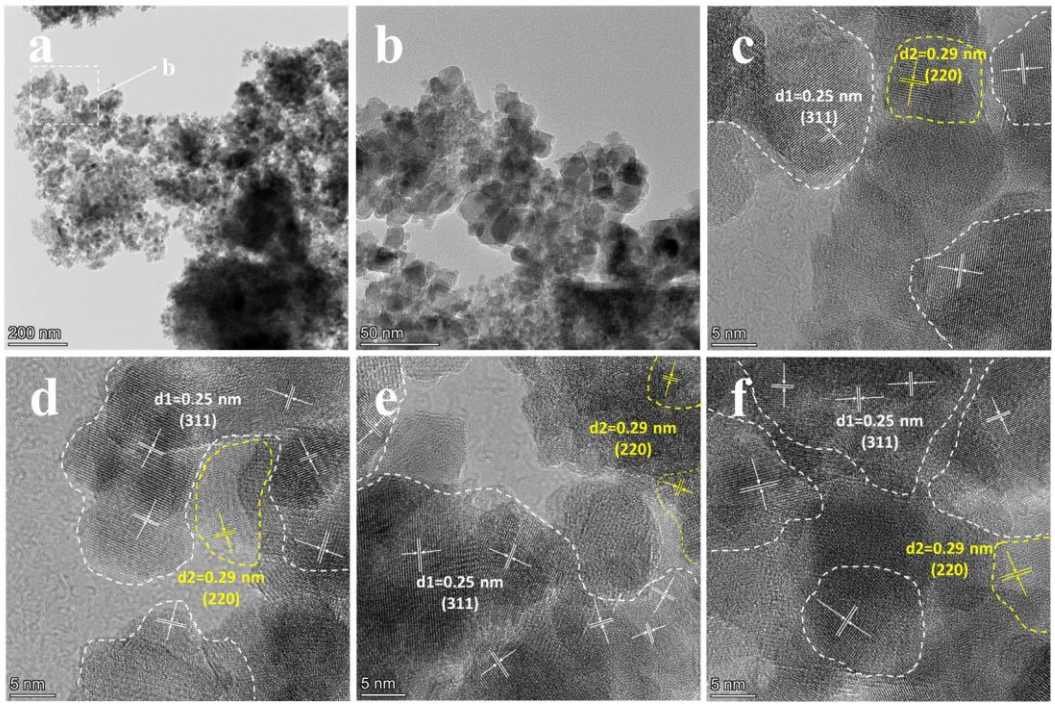

Figure S4. (a-b) TEM images, (c-f) HRTEM images of $Mn_{0.5}Fe_{2.5}O_4$-P.

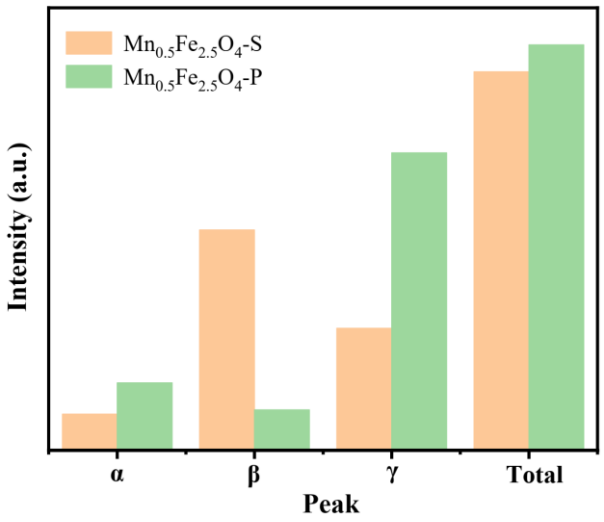

Figure S5. Integral area of H_2 consumption on different peaks over the $Mn_{0.5}Fe_{2.5}O_4$ catalysts.

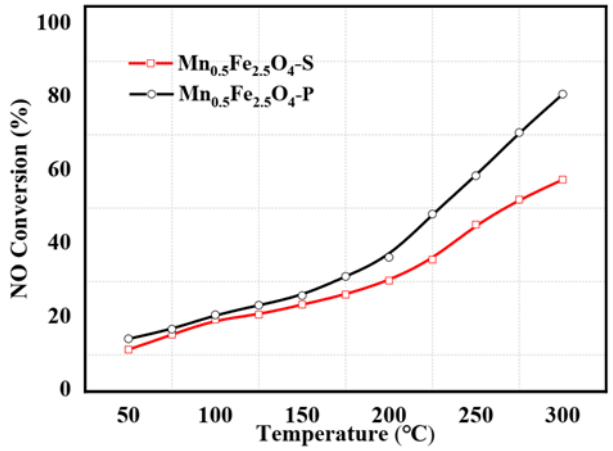

Figure S6. NO conversion over $Mn_{0.5}Fe_{2.5}O_4$ catalysts.

In order to make sure the best catalytic performance, the performance of mesoporous Fe-Mn nanosphere with different proportions were measured as shown in Figure S7. The $Mn_{0.25}Fe_{2.75}O_4$ catalyst exhibited an unsatisfactory low-temperature catalytic efficiency, achieving more than 90% NO_x conversion at a high temperature of 200 °C. With the increase of Mn ratio to 0.5, the catalytic performance of $Mn_{0.5}Fe_{2.5}O_4$ sample was boosted with improved low-temperature catalytic activity and widened temperature window. With the further increasing of Mn content to 0.75, the $Mn_{0.75}Fe_{2.25}O_4$ sample showed a sharply decreased low-temperature catalytic performance. Therefore, the $Mn_{0.5}Fe_{2.5}O_4$ spinel was used as the reference object to explore the influence of morphology on the catalytic performance.

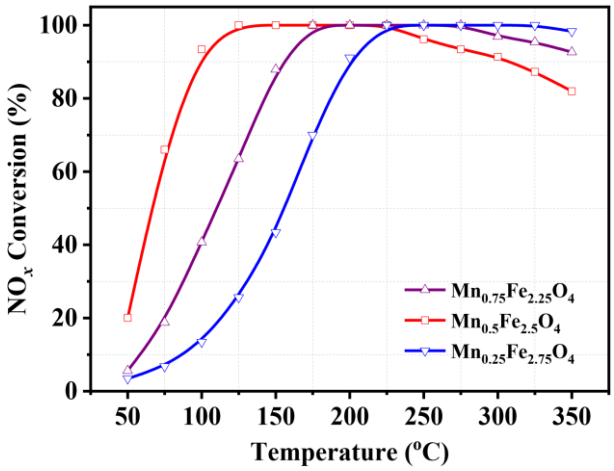

Figure S7. NO*x* conversion over different Mn-Fe ratio Reaction conditions: [NO] = [NH_3] = 500 ppm, [O_2] = 5 vol %, Ar balance, and GHSV = 50000 h^{-1}

The influence of internal diffusion and external diffusion were studyed by changing the particle size of the catalyst and total gas flow rate (TGFR). As shown in Figure S8., the $Mn_{0.5}Fe_{2.5}O_4$-S_S (catalyst size is 40 – 60 mesh) exhibited the equivalent catalytic performance with $Mn_{0.5}Fe_{2.5}O_4$-S_L (catalyst size is 20 – 40 mesh) under the same GHSV of 50000 h^{-1}. As for $Mn_{0.5}Fe_{2.5}O_4$-P, the catalytic activity of small size sample was slight higher than that of large size sample especially in middle temperature region, while the difference between them is inconspicuous. Based on the results, it could be affirmed that the influence of internal diffusion has been eliminated in our experimental condition. In addition, when the TGFR increased from 100 mL·min^{-1} to 150 mL·min^{-1} (Figure S9), the NO conversion slightly increased in the middle temperature stage. However, the NO conversion increased a lot in the whole temperature when the TGFR increased to 200 mL·min^{-1}, which was caused by the eliminated external diffusion. With further increasing to 250 mL·min^{-1}, the catalytic activity was almost unchanged. The result demonstrated that the selected reaction condition (200 mL·min^{-1}) could fully eliminated the external diffusion effect.

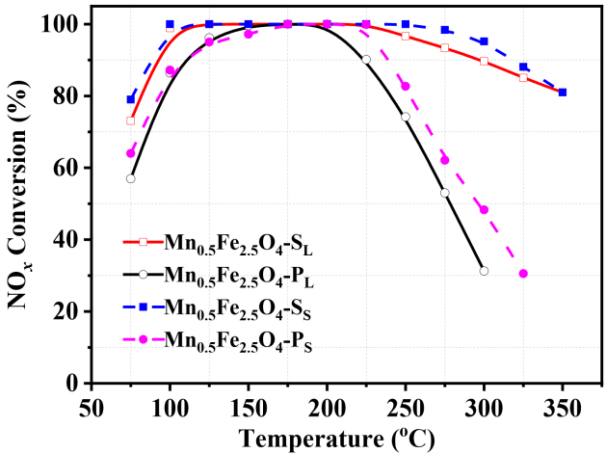

Figure S8. NO*x* conversion of $Mn_{0.5}Fe_{2.5}O_4$ with different catalysts article size.

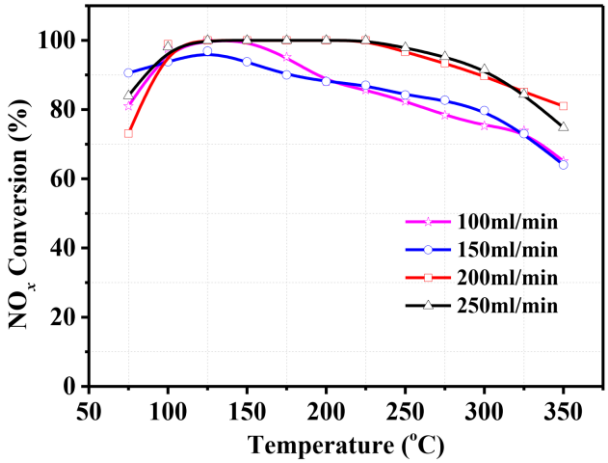

Figure S9. NO*x* conversion of $Mn_{0.5}Fe_{2.5}O_4$-S catalysts over different total flow rate.

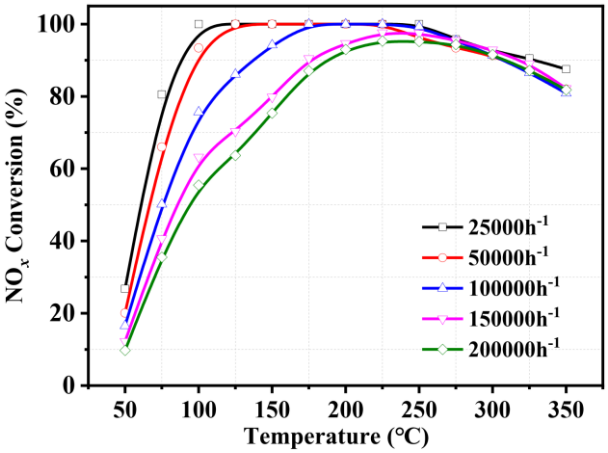

Figure S10. NO*x* conversion over different GHSV of Mn0.5Fe2.5O4-S.

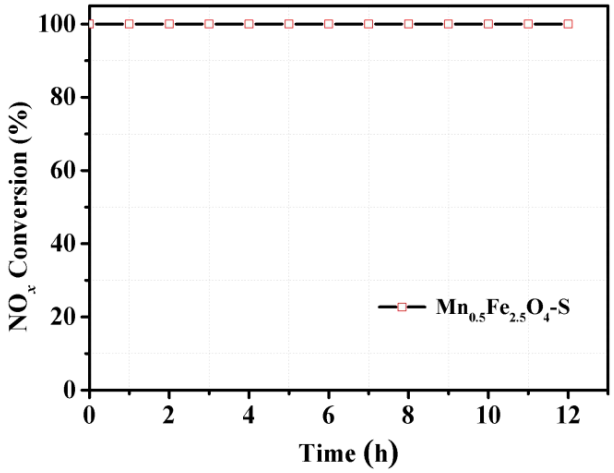

Figure S11. NO*x* conversion over $Mn_{0.5}Fe_{2.5}O_4$-S Reaction conditions: [NO] = [NH_3] = 500 ppm, [O_2] = 5 vol %, Ar balance, and GHSV = 50000 h^{-1}

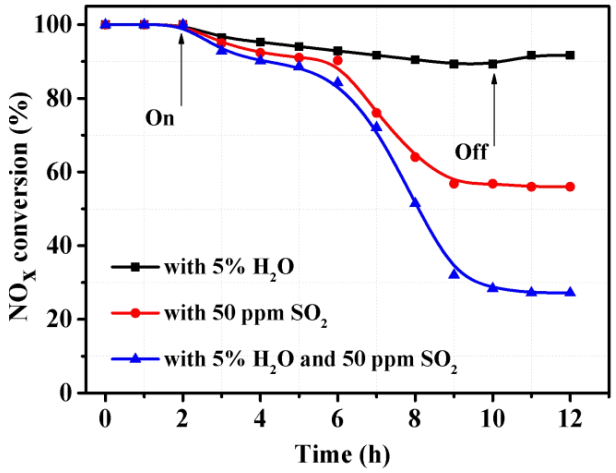

Figure S12. Durability tests of the $Mn_{0.5}Fe_{2.5}O_4$-S catalyst at 175 ºC. Reaction conditions: [NO] = [NH_3] = 500 ppm, [O_2] = 5 vol %, [SO_2] = 50 ppm (when used), [H_2O] =5 vol% (when used), balanced with Ar, GHSV = 50 000 h^{-1}

As shown in Figure S13, the monolithic catalysts exhibit an integral tube-like structure with a 1 mm inner diameter channel in the center, which make sure the gases smoothly through the catalysts. Similarly, the monolithic catalyst was put into the U-tube quartz to test its NH_3-SCR activity. Because there is quarter pseudo-boehmite in the monolithic catalysts as the support, the GHSV was decreased from 50000 h^{-1} to 36000 h^{-1} to insure the same mass with powder catalyst.

As predicted, the monolithic catalysts (denoted as $Mn_{0.5}Fe_{2.5}O_4$-S_M) exhibited much lower SCR performance than that of tableting catalyst (denoted as $Mn_{0.5}Fe_{2.5}O_4$-S_T) especially the low-temperature activity (Figure S13). Such results mainly due to the decreased contact area between reactant gases and catalysts. In order to verify the De-NOx activity of monolithic catalysts under real environments, the SCR stability performance of $Mn_{0.5}Fe_{2.5}O_4$-S_M was measured in the presence of 5% H_2O and 50 ppm SO_2 at 175ºC. When 50 ppm SO_2 and 5% H_2O were simultaneously added to reaction system, the NO_x conversion decreased from 70% to 50% within 2 hours and did not changed in the next 6 hours (Figure S14). After cutting off H_2O and SO_2, the catalytic activity slightly increased, suggesting that the passivation influence could be eliminated partly. Compared with the $Mn_{0.5}Fe_{2.5}O_4$-S_T sample, the $Mn_{0.5}Fe_{2.5}O_4$-S_M catalyst not only exhibited lower catalytic activity decline but could recover partially after stopping H_2O and SO_2, demonstrating its better resistance to water and sulfur. The phenomenon should be attributed to the existing of pseudo-boehmite and its monolithic structure. The $Mn_{0.5}Fe_{2.5}O_4$-S spinel catalysts exhibited good SCR performance in the real environment, which could be a promising candidate for the industry application.

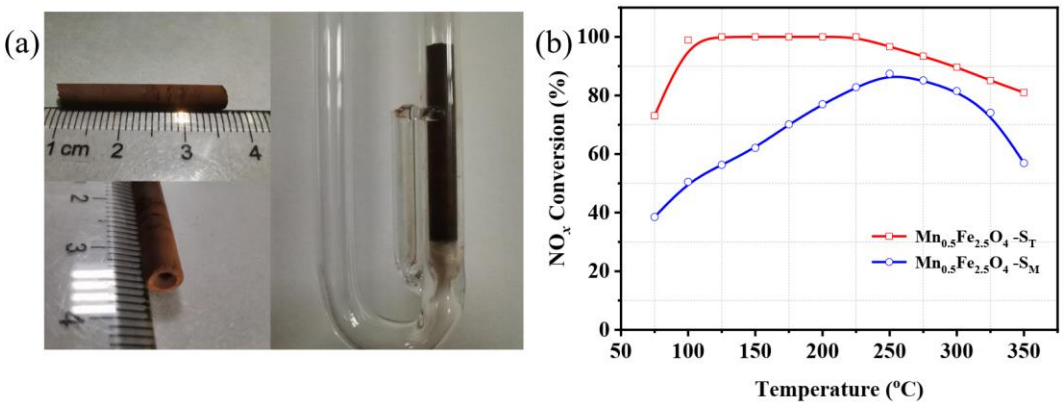

Figure S13. (a) Images of the monolithic catalysts and U-tube quartz reactor, (b) NO_x conversion over $Mn_{0.5}Fe_{2.5}O_4$-S_M and $Mn_{0.5}Fe_{2.5}O_4$-S_T catalysts.

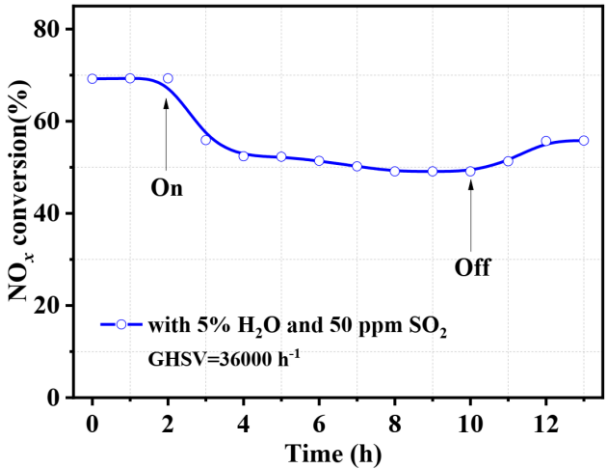

Figure S14. Durability tests of the $Mn_{0.5}Fe_{2.5}O_4$-S_M catalyst at 175 °C. Reaction conditions: [NO] = [NH_3] = 500 ppm, [O_2] = 5 vol %, [SO_2] = 50 ppm (when used), [H_2O] =5 vol% (when used), balanced with Ar, GHSV = 50 000 h^{-1}

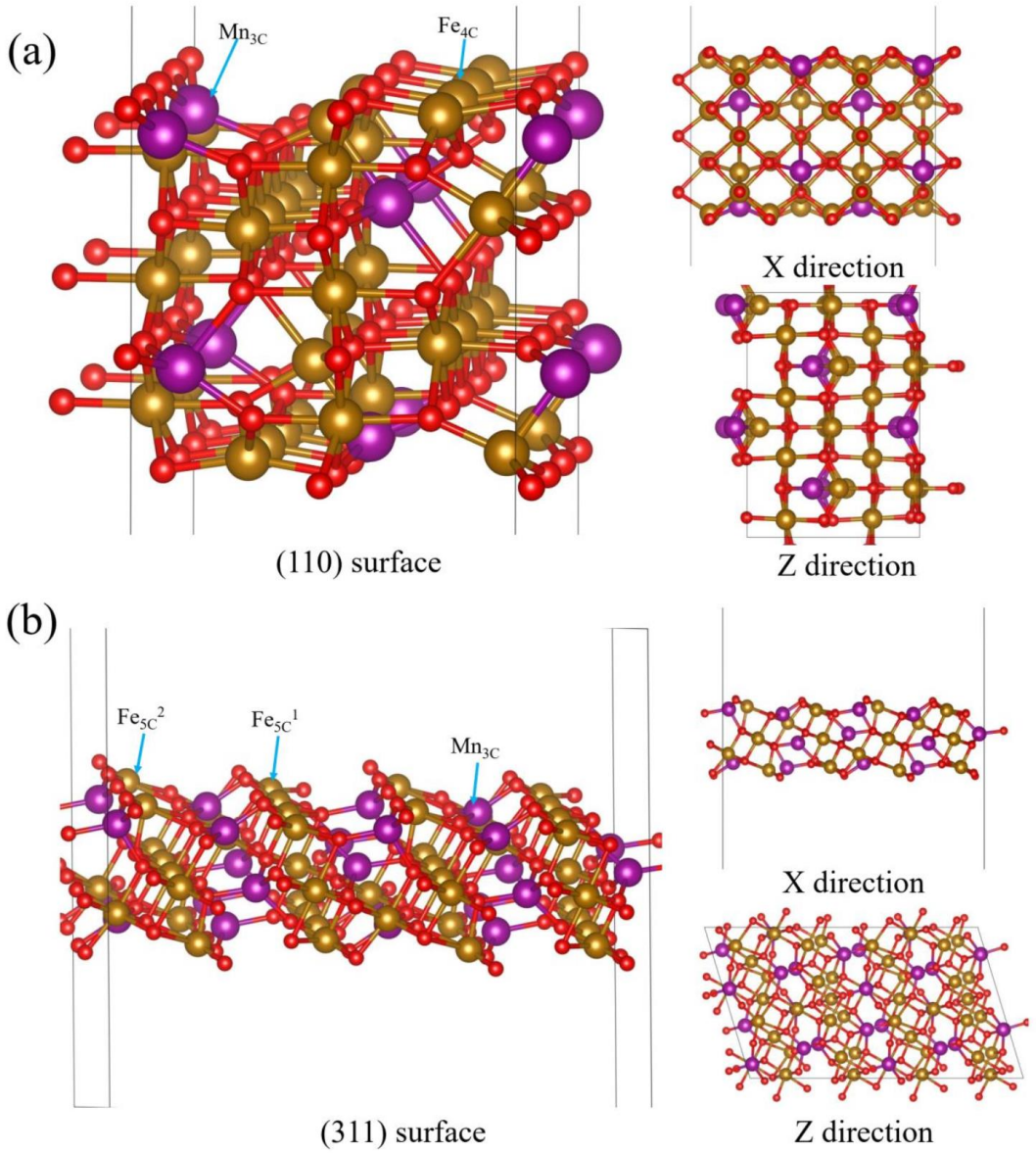

Figure S15. The DFT calculation model of $Mn_{0.5}Fe_{2.5}O_4$ in (a) (110) plane and (b) (311) plane. Golden, purple, and red balls represent Fe, Mn, and O atoms, respectively, and this color scheme will be used throughout. Fe_{4C}/Fe_{5C} stands for the four-coordinated/five-coordinated Fe atom, Mn_{3C} stands for the three-coordinated Mn atom, and two different surface Fe_{5C} atoms exist in (311) surface, noted as Fe_{5C}^1 and Fe_{5C}^2.

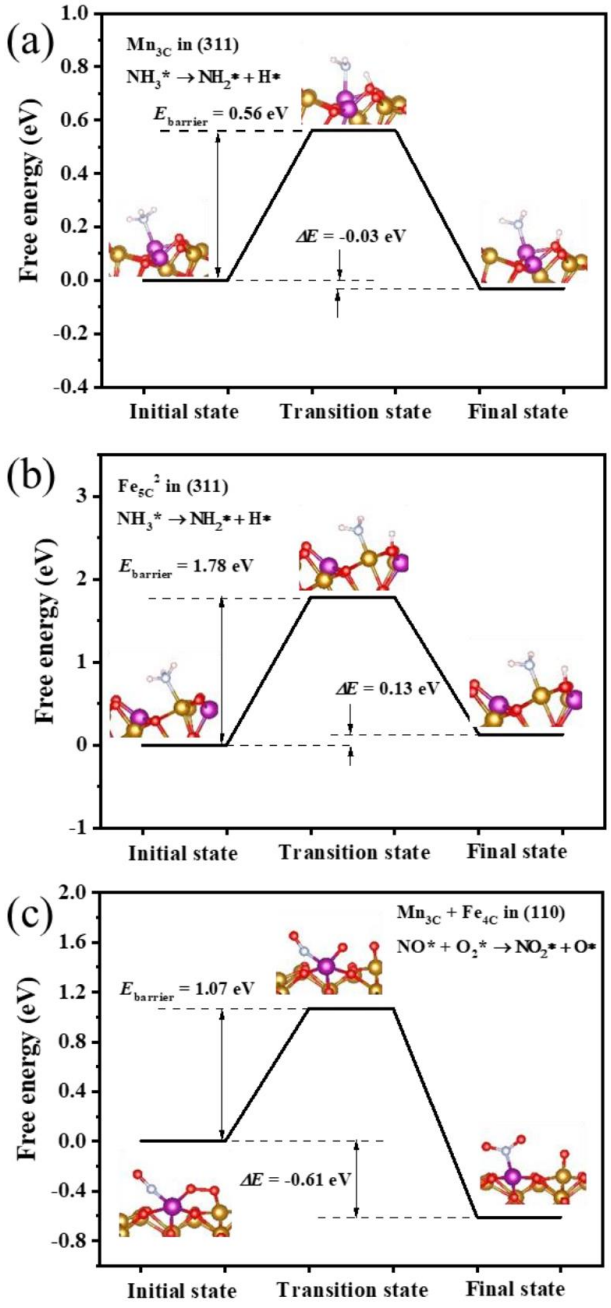

Figure S16. Energy profiles of initial state, transition state, and final state of NH_2 (a-b) and NO_2 (c) formation on the (110) and (311) plane of $Mn_{0.5}Fe_{2.5}O_4$.

Table S1. Crystallite size calculated by the Scherrer's formula and Lattice parameter of catalysts.

Simple	Crystallite Size（nm）	Lattice parameter（Å）
Fe_2O_3-S	15.5	8.36038
$Mn_{0.5}Fe_{2.5}O_4$-S	12.1	8.35699
$Mn_{0.5}Fe_{2.5}O_4$-P	14.4	8.35842

Table S2. H_2 consumption of different peaks over $Mn_{0.5}Fe_{2.5}O_4$ catalysts.

Sample	H_2 consumption (mmol $H_2 \cdot g^{-1}$)			
	α	β	γ	Total
$Mn_{0.5}Fe_{2.5}O_4$-S	1.7	10.1	5.5	17.3
$Mn_{0.5}Fe_{2.5}O_4$-P	3.2	1.9	13.5	18.6

REFERENCES

(1) Liu, B.; Li, X.; Zhao, Q.; Hou, Y.; Chen, G. Self-templated formation of $ZnFe_2O_4$ double-shelled hollow microspheres for photocatalytic degradation of gaseous o-dichlorobenzene. J. Mater. Chem. A. **2017**, 5 (19), 8909-8915,doi:10.1039/c7ta02048a.

(2) Yang, S.; Yan, N.; Guo, Y.; Wu, D.; He, H.; Qu, Z.; Li, J.; Zhou, Q.; Jia, J. Gaseous elemental mercury capture from flue gas using magnetic nanosized $(Fe_{3-x}Mn_x)_{1-\delta}O_4$. Environ. Sci. Technol. **2011**, 45 (4), 1540-1546,doi:10.1021/es103391w.

(3) Mu, J.; Li, X.; Sun, W.; Fan, S.; Wang, X.; Wang, L.; Qin, M.; Gan, G.; Yin, Z.; Zhang, D. Enhancement of Low-Temperature Catalytic Activity over a Highly Dispersed Fe–Mn/Ti Catalyst for Selective Catalytic Reduction of NO_x with NH_3. Ind. Eng. Chem. Res. **2018**, 57 (31), 10159-10169,doi:10.1021/acs.iecr.8b01335.